ALJEST

Kinetic and thermodynamic studies of methylene blue adsorption on sorghum stems

N. Sifoun [(1,2)], A-R. Yeddou *[(3)], L-H. Nouri [(1,4)], A. Chergui [(3)], B. Nadjemi [(3)]

[(1)] Research Laboratory of Food Technology, Faculty of Engineering Sciences, M'Hamed Bougara University, Boumerdes 35000, Algeria.
[(2)] Institut of technology I.T, University Akli Mohand Oulhadj of Bouira U.A.M.O, Rue Drissi Yahia Bouira 10000, Bouira, Algeria
[(3)] Laboratory of Study and Development of Techniques of Water Treatment and Environmental Management - L.E.D.T.E.G.E, Department of Chemistry, E.N.S Kouba, BP 92 Kouba 16308, Algiers, Algeria
[(4)] Department of Process Engineering, Faculty of Engineering Sciences, M'Hamed Bougara University of Boumerdes U.M.B.B, Avenue de l'Indépendance 35000, Boumerdes, Algeria

*Corresponding author: n.sifoune@univ-boumerdes.dz

ARTICLE INFO

ABSTRACT/RESUME

Abstract: The Raw Sorghum stems have been studied as to adsorb Methylene Blue from aqueous solution by batch technique. The effects of different parameters such as adsorbent dose, initial pH, ionic strength, contact time and dye initial concentration have been studied. To describe the adsorption kinetics, five models were applied. Kinetic parameters for each adsorption kinetic equation were calculated and discussed. The experimental isotherm data were analyzed using three models. The recovery of methylene blue adsorption has been exceeded 80%. The pseudo-second order kinetic model adequately describes the kinetic data with high determination coefficient ($R^2=0.99$). Langmuir isotherm model fits better than Freundlich and Temkin models for all temperatures studied, and the maximum methylene blue uptake was observed as 27.67 mg/g at 313 K. The estimated values for $\Delta G°$ were -2.56, -3.31and -3.78 kJ/mole at 295, 303 and 313 K respectively. The enthalpy changes $\Delta H°$ and entropy $\Delta S°$ of adsorption were 17.19 kJ/mole and 67.24 J/mole.K, respectively.

I. Introduction

The removal of pollutants, like dyes and pigments, is becoming a significant environmental problem due to their widespread use in many industrial applications. Dyes are widely used in manufacturing processes, consequently they are usually present in the effluent water of many industries, such as textiles, leather, pulp mill paper, printing, dye synthesis and cosmetics [1]. For example, methylene blue, red Congo, methyl orange and reactive blue 19 are used in the textile industry. The colored wastewater is characterized by a high chemical and biological oxygen demands, suspended solids and toxic compounds, which makes them difficult to biodegrade [2]. The presence of dyes in discharged wastewater, even at low concentrations, cause serious harm to the aquatic life, inhibit to aquatic life and pose acute problems for the ecological system [3,4]. The removal of dyes from wastewater has received considerable attention over the past decades [5]. The most commonly proposed processes are chemical coagulation [6], electro-coagulation [7], filtration membranes [8], oxidation and ozonation [9], ion exchange [10], adsorption [11,12], photocatalytic degradation [13] and biological treatments [14].

Adsorption method is considered to be one of the most promising techniques for water and wastewaters treatment [15], because of its simplicity, high efficiency, and wide-ranging availability [16]. Several materials as polymers [17], metal oxides [18], carbon nanotubes [19], nanoparticles and nanocomposites [20], rubber tire

[21], graphene oxide [22], biological biomass [23] and activated carbon [24] have been used for the rapid removal of harmful impurities from the aqueous solutions. Activated carbon is the most popular adsorbent for wastewater treatment. It presents diverse advantages: high specific surface areas and large porous volumes to adsorb high quantity of pollutants [25]. However, it is an expensive material because of the chemical and/or physical treatments used for its synthesis and the need for it regeneration, which make its application less economically attractive on an industrial scale [26, 27].

To reduce the cost of adsorption, studies have focused on the use of inexpensive or zero-cost adsorbents such as forestry and agricultural solid byproducts. These no-conventional wastes, abundant have been proved the success for organic and inorganic pollutants removal. Recently, a number of low-cost adsorbents have been examined [26-30]. Many have been used for the removal of dyes. We cite sawdust [31], hulls of tropical almonds [25], date and palm waste [32], fallen phoenix leaves [33] and pistachio hull powder [34]. Sorghum is cultivated in different region in Algeria especially in the Sahara (southern). The particularity of this cultivar lies to it growth in hyper arid ecosystem where the maturity temperature is very high and it irrigation using saline underground water. It is also known for its high drought resistance and capacity to grow using low-input agricultural fertilizers [35]. Sorghum is grown for its grain for human consumption. Until recently, sorghum stalks of locally cultivated varieties appeared mainly as a residue used for livestock feed.

The purpose of the present work was to valorize stems Sorghum of southern of Algeria as biosorbent for dyes removal from aqueous solutions in batch system. Methylene blue was selected as a model compound in order to evaluate the capacity of this agricultural waste for the elimination of dyes. The study includes an evaluation of the effects of various operational factors to optimize the biosorption efficiency of material such as: amount of adsorbent, pH, ionic strength, contact time, and dye initial concentration. The adsorption kinetic models and equilibrium isotherm models related with the process were also studied. Finally, the thermodynamic parameters corresponding to the adsorption process were determined and discussed.

II. Materials and methods
II.1. Biosorbent preparation
Stems of sorghum plants were obtained from In Salah situated in Tidikelt (south east region in Algeria). Most sorghum cultivar sgrown in this region belong to the species Sorghum bicolor (L.) Moench. The stems were dried in the open air. Prior touse, the stems were cut in to pieces, milled by

IKA labotechnik A10 and sieved in particles size range from 0.50 to 0.63 mm. The stem fibers were intensively washed with distilled water and dried at 105 °C for 48 h in an air circulating oven. The obtained sorghum fibers present our raw adsorbent and was noted RSF. Thereafter, the biosorbent was stored in a desiccator for further experimental use.

The determination of the pH_{pzc} value of RSF was as follows: 50 mL of 0.01 M aqueous NaCl solution were placed in closed flacons. The pH was adjusted to a value between 2 and 11 by adding HCl or NaOH solutions (0.01 N). Then, a RSF mass of 0.15 g was added to each solution and thefinal pH measured after 24 h using a Jenway 3010 pH-meter. The pH_{pzc} is the point where the curve $pH_{initial}$ vs pH final crosses the line $pH_{initial} = pH_{final}$ [36].The photomicrography of the exterior surface of RSF was obtained by Scanning electron microscopy SEM (Quanta FEG 250, FEI). FT-IR spectrum of RSF was recorded on a Bruker FT-IR spectrometer Alpha instrument (4000-400 cm^{-1}region).

II.2. Batch biosorption experiments
To determine adsorption capability of the biosorbents, batch adsorption experiments were conducted by using aqueous solution of Methylene Blue (MB).The stock solution of MB with a concentration of 500 mg/L was prepared by dissolving a quantity of MB powder ($C_{16}H_{18}N_3SCl$, 98.5% purity, Fluka) in distilled water. The working MB solutions were prepared by diluting the stock solution to give the appropriate concentrations (C_0).

For the study of the influence of the various parameters, all adsorption experiments were carried out by mixing 100 mL of MB solution at initial concentration C_0 with an appropriate dried biosorbent mass at room temperature. The tested parameters were biosorbent dose, initial solution pH, NaCl and $CaCl_2$ ionic strength, contact time and initial MB concentration. The pH solution was adjusted by adding micro volumes of either 0.1 M NaOH or 0.1 M HCl.

For evaluating adsorption kinetic, the experiments were conducted at room temperature by using 100 mL of MB solutions at initial concentrations: 25, 50 and 100 mg/L with biosorbent dose equal to 4g/L.

The adsorption isotherms were conducted by shaking for 24 hours and using different initial concentrations of MB between 10 and 100 mg/L at adsorbent mass equal to 0.2 g for 100 mL of solution.

In all experiments, solutions were shaken using a magnetic stirrer at 150 rpm for different periods of time contacts. For predetermined time interval, a small portion of samples were taken and the concentration of MB remained. Concentrations of MB at time t (C_t) and concentrations of MB at equilibrium time (C_e) were then measured using

UV/visible spectrophotometer (UV-1800 SHIMADZU) at 664 nm.

The percentage of MB adsorbed (%) and the amount of MB adsorbed at time t (mg/g) were calculated using Eq. 1 and Eq. 2 respectively.

$$Removal\ (\%) = \frac{C_0 - C_t}{C_0} \times 100 \qquad (1)$$

$$q_t(mg/g) = \frac{C_0 - C_t}{m} \times V \qquad (2)$$

The amount of MB adsorbed onto biosorbent at equilibrium (mg/g) was calculated using the following expression Eq. 3:

$$q_e(mg/g) = \frac{C_0 - C_e}{m} \times V \qquad (3)$$

Where C_0 was concentration of MB at initial time (mg/L), V is the volume of the MB solution (L), m is the dried mass of RSF biosorbent (g).

III. Results and discussion
III.1. The RSFcharacterizations

Figure 1 illustrates the pH_{pzc} of RSF, which was found to be 5.78. Therefore, the surface of RSF acquired a positive charge below 5.78, while it was negatively charged above this pH value. The Scanning electron micrographs of RSF are shown in **Figure 2**. As it can be seen, RSF has an irregular texture with a considerable numbers of pores where there is a great possibility for the MB adsorption. The FT-IR spectra of RSF represented by **Figure 3**, displays a number of absorption peaks identifying some functional groups. The intense absorption bands at 3340.78 cm^{-1} indicate the existence of hydroxyl groups on the surface of RSF. This band is associated with the vibrations of the linked hydroxyl groups in cellulose and lignin, and adsorbed water on the RSF surface. The peaks at 2905.51 and 1316.36 cm^{-1} are assigned to the stretch and bending vibration of the C-H bond in the methyl groups -CH$_3$, respectively. The peak at 1729.63 cm^{-1} is characteristic of carbonyl C=O stretching and can be attributed to the hemicellulose and lignin. The absorption bands corresponding to 1602.40-1511.97 cm^{-1} represents C=C stretching in aromatic region. The peak at 1426.44 cm^{-1} can also attribute to the stretch vibration of C-O associated with the carboxyl group or represent C-C stretching vibration of carboxylic acid and alcohols. The broad absorption bands observed at 1237.45,
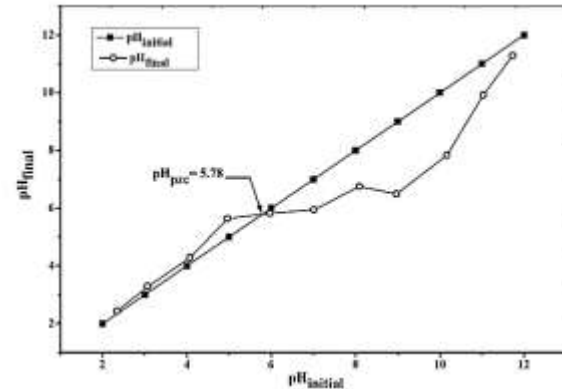
1159.00 and 1031.41cm^{-1} can be assigned to C-O [26].

Figure1.*Determination of pH_{pzc}.*

III.2. Effect of RSF adsorbent dose

The amount of used adsorbent plays an important role in adsorption process. **Figure 4** illustrates the variation of percentage removal and adsorption capacity of MB by varying RSF dose from 1 to 8 g/L. It is shown that the increase in RSF dose has a consequence enhancement of MB removal from 87 to 98.7 %, corresponding to a decrease of adsorption capacity from 21.76 to 3.00 mg/g. The removal enhancement can be due to the availability of more adsorption active sites and to the increase in surface area. However, the adsorbed capacity decrease may be due to the over lapping and accumulation of binding sites [26,37].

III.3.Effect of initial solution pH

The pH plays an important role in adsorption process. **Figure 5** shows the effect of this parameter on the percentage removal and adsorption capacity of MB onto RSF. From the figure, the amount adsorbed of MB increases from 4.99 to 6.00 mg/g when solution pH increases from 3.24 to 5.16, corresponding to an increasing removal percentage from 79 to 96 %. And for pH range from 5.16 to 10.00, there is no significant change. At acidic pH range (lower than pH_{pzc}), lower MB adsorption is probably due to the presence of H^{+} ions excess competing with the cation groups on the MB for adsorption sites. At basic pH range (higher than pH_{pzc}), the RSF surface is negatively charged, which favors electrostatic interactions with MB (cationic dye) molecules [38]. This, however, didnot explain the slight decrease of dye adsorption at higher pH values [31]. MB solution has natural pH between 6 and 7 and at this pH, adsorption of MB dye is maximum with the RSF. Hence, pH of MB dye solution has not been varied in further experiments.
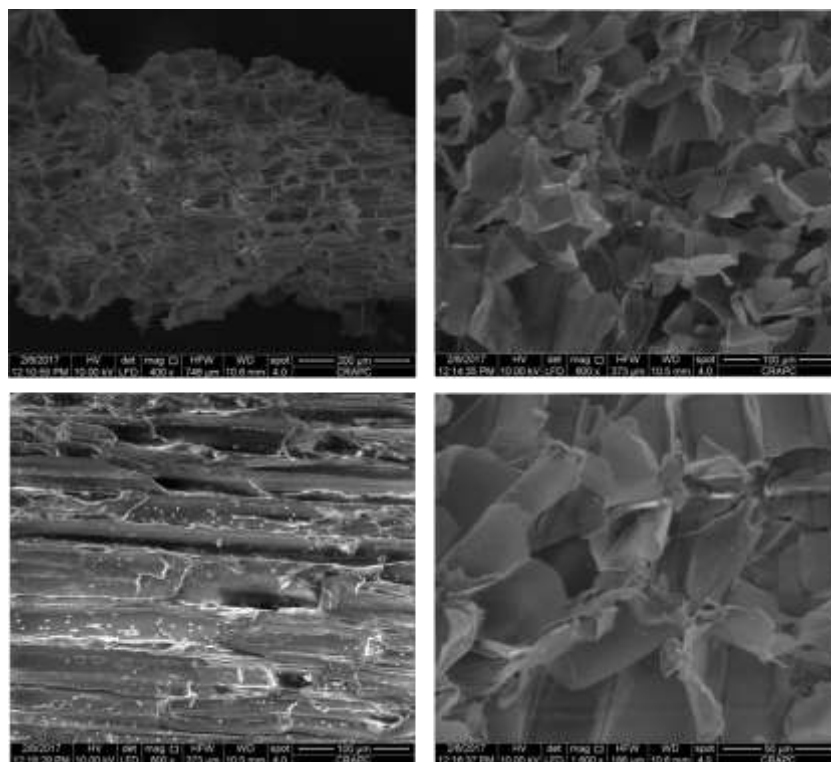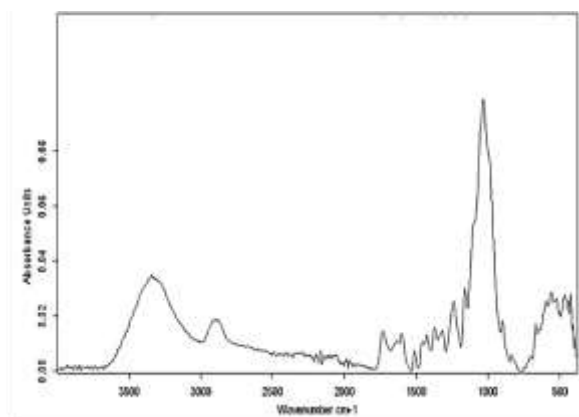
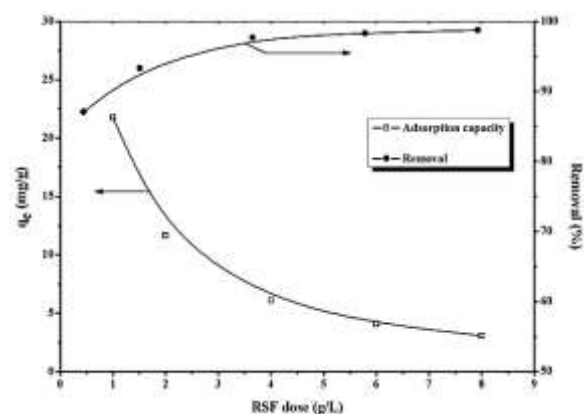*Figure 2. SEM images of RSF.*

Figure 3.FT-IR spectrum of RSF.

Figure 4. Effect of the RSF dose on the adsorption capacity and percentage removal of MB(particle size= 0.50-0.63 mm, C_0= 25 mg/L,time= 24 h, pH solution).

III.4. Effect of ionic strength

The influence of salt concentration on the adsorption ability of RSF was studied by addition of NaCl and CaCl$_2$ to the MB solution in range from 0 to 0.1 mole/L. As seen in **Figure 6 (a)**, when the salt concentration increased from 0 to 0.1 mole/L, the value of adsorption capacity decreased from 6.1 to 4.28 and 3.44 mg/g for NaCl and CaCl$_2$, respectively. From **Figure 6 (b)**, the same thing was observed for the MB removal, which decreased from 97.6 to 68.47 and 55.17 % for NaCl and CaCl$_2$, respectively. The decreasing adsorption efficiency with the salt concentrations increasing can be related to the competitive effect between

MB ions and cations from the salts (Na$^+$ and Ca^{2+}) for the sites available for the adsorption process [39].The influence of NaCl on removal of MB was weaker than CaCl$_2$ because unit mole univalent Na$^+$ contributed less positive charges than unit mole divalent Ca^{2+} [40].

III.5. Effect of initial concentration of MB

This study was performed by changing the initial concentration of MB in the range of 10-100 mg/L for an RSF dose equal to 4 g/L.The results
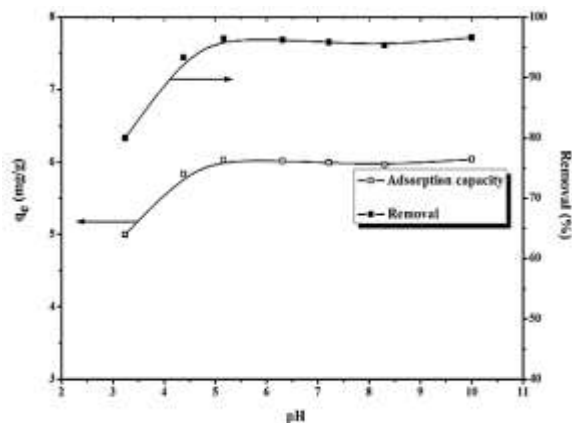
Figure 5. *Effect of the initial pH on adsorption capacity and percentage removal of MB onto RSF (particle size= 0.50-0.63 mm, C_0= 25 mg/L, RSF dose= 4 g/L, contact time= 24 h).*
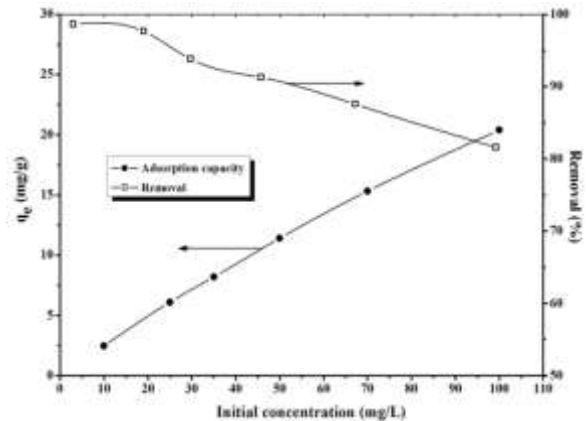

Figure 6. *Effect of ionic strength on (a) adsorption capacity and (b) percentage removal of MB onto RSF (particle size= 0.50-0.63 mm, C_0= 25 mg/L, RSF dose= 4 g/L, pH solution, contact time= 24 h).*

presented in **Figure 7**, show that adsorption capacity increase from 2.4 to 20.4 mg/g with increasing in initial concentration of MB from 10 to 100 mg/L. In this range of initial dye concentration, the removal decreased from 96.4 to 81.58 %. At higher concentrations, the excess dye molecules are not adsorbed by the RSF, due to the saturation of the limited binding sites on RSF surface [41].

III.6. Effect of contact time

The contact time, in any water treatment process, is one of the operating parameters that are given great consideration. The effect of this important parameter was investigated for three initial concentration of MB (25, 50 and 100 mg/L) and the results are shown in **Figure 8**. As shown in this figure, it can be clearly seen that the amount MB

Figure 7. *Effect of MB initial concentration on the adsorption of MB onto RSF (particle size = 0.50-0.63 mm, RSF dose= 4 g/L, pH solution, contact time= 24 h).*
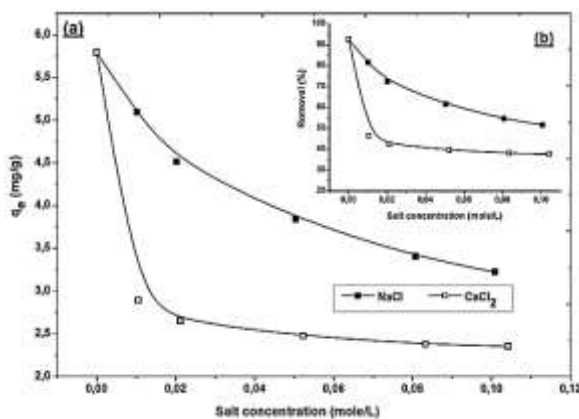
Adsorbed onto RSF, increases with increasing contact time and in the first 20 min, the initial rate of adsorption was greater for higher initial MB concentration. For all initial MB concentration, three important phases in the adsorption process can be observed. In the first phase, the adsorption rate is rapid. About 85, 62 and 48 % of the removal was achieved after 20 min for initial concentration 25, 50 and 100 mg/L, respectively. In the second phase, the adsorption begins to slow and there be no significant increase. In the third phase, the equilibrium is reached and the adsorption capacity does not vary.
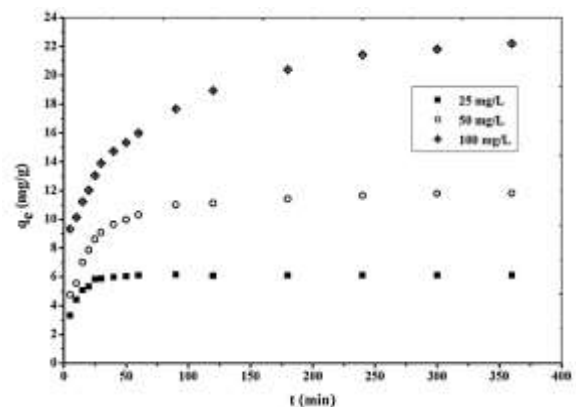

Figure 8. *Effect of contact time on the adsorption of MB onto RSF for different initial concentration (particle size= 0.50-0.63 mm, RSF dose= 4 g/L, pH solution).*

It can also be observed that the equilibrium time was increased with increasing initial MB concentration. The time required to achieve equilibrium was 30, 90 and 240 min for initial MB

concentration 25, 50 and 100 mg/L, respectively. An increase of MB concentration accelerates the diffusion of MB from the solution onto RSF due to the increase in driving force of the concentration gradients [42].

III.7. Kinetic studies

The kinetic study is important for the adsorption process because it describes the uptake rate of adsorbate, and controls the residual time of the whole process. Tree kinetic models namely the pseudo-first order, pseudo-second order and Elovich are selected in this study for describe the adsorption process.

The pseudo-first order equation [43] is given in equation Eq. 4:

$$\ln (q_e - q_t) = \ln q_e - K_1 \cdot t \qquad (4)$$

The pseudo-second order model [43] is expressed by the equation Eq. 5. For the pseudo-second order, the initial adsorption rate h (mg/g.min) is expressed by the equation Eq. 6.

$$\frac{t}{q_t} = \frac{1}{K_2 \cdot q_e^2} + \frac{1}{q_e} \cdot t \qquad (5)$$

$$h = K_2 q_e^2 \qquad (6)$$

The Elovich model [44] is given by the simplify equation Eq. 7:

$$q_t = \frac{1}{\beta} \ln (\alpha\beta) + \frac{1}{\beta} \ln t \qquad (7)$$

Where K_1 is the rate constant of the pseudo-first order kinetic (min^{-1}), K_2 is the rate constant of the pseudo-second order kinetic (g/mg.min), α (mg/g.min) is the initial rate constant and β (mg/g) is the desorption constant during any one experiment.

The slope and intercept of the plots of ln (q_e - q_t) versus t was used to determine the first-order rate constants K_1 and q_e. The slope and intercept of the plot of t/q_e versus t was used to determine the second-order rate constants K_2 and q_e. The constants α and β for Elovich model were determinate by the slop of q_t against ln t.

The kinetic constants, (q_{e1}, K_1) for pseudo-first order, (q_{e2}, K_2) for pseudo-second order and (α, β) for Elovich models are determined and the corresponding linear regression coefficient (R^2) values are given in **Table 1**. We can note, from the results, that the pseudo-second order model fits better than the pseudo-first order and Elovich models with higher determination coefficients ($R^2 >$ 0.99). The experimental adsorption capacity ($q_{e,exp}$) values are very close to the model calculated values (q_{e2}), verifying the high correlation of adsorption to the pseudo-second order model.

The intraparticule diffusion model can be useful for identifying adsorption mechanisms, the reaction pathways and predicting the rate controlling [44]. The linearized form is presented by Eq. 8, and the constants were determined by the plot of q_t versus $t^{1/2}$ [31].

$$q_t = K_{in} \cdot t^{1/2} + C \qquad (8)$$

Where K_{in} is the intraparticle diffusion rate constant (mg/g.min$^{1/2}$). Values of intercept C gives an idea about the thickness of boundary layer. This is attributed to the instantaneous utilization of the most readily available adsorbing sites on the adsorbent surface.

As seen from **Figure 9**, the plots of q_t against $t^{1/2}$ are not linear over the whole time range and give two straight-line with different slopes and intercepts values. The values of $K_{in(i)}$, C_i and the corresponding linear regression coefficient R_i^2 obtained from the first and second linear portions are listed in **Table 1**. The values of C_i are different from 0 and the straight-line does not pass through the origin implying that the adsorption rate of MB on RSF is not only controlled by the intraparticle diffusion but also by the diffusion in the boundary layer [31,40].
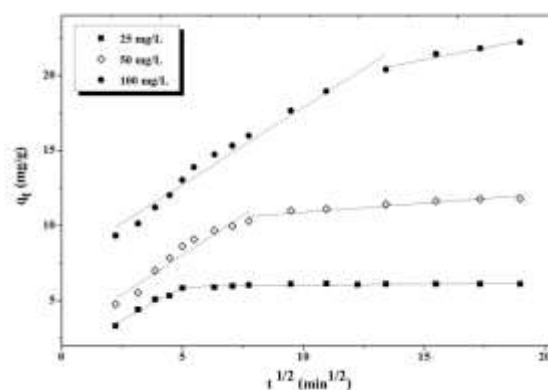
Figure 9. *Adsorption kinetics of MB onto RSF: intraparticle diffusion.*

III.8. Adsorption isotherms

Adsorption isotherm was used to obtain information about the mechanism and the interaction between the RSF and MB at a given temperature (295, 303 and 313 K). The equilibrium adsorption experiments were analyzed by fitting them to tree known and widely applied isotherm models equations Langmuir, Freundlich and Temkin.

- *Langmuir isotherm*

The linear form of the Langmuir isotherm is represented by the following equation:

$$\frac{C_e}{q_e} = \frac{1}{q_m} C_e + \frac{1}{K_L q_m} \qquad (9)$$

Table 1. *Adsorption kinetic parameters for adsorption of MB onto RSF for different initial concentrations.*

Initial concentration (mg/L)		25	50	100
$q_{e,exp}$ (mg/g)		**6**	**11.25**	**21.72**
Pseudo-first order	K_1 (min^{-1})	0.299	0.081	0.049
	q_{e1} (mg/g)	6.245	7.523	26.85
	R^2	0.893	0.977	0.90
Pseudo-second order	K_2 (g/mg.min)	0.039	0.008	0.003
	q_{e2} (mg/g)	**6.100**	**12.155**	**23.100**
	R^2	**0.999**	**0.999**	**0.997**
	h (mg/g.min)	1.484	1.182	1.600
Elovich	α (mg/g.min)	457.664	8.357	7.224
	β (mg/g)	1.923	0.589	0.298
	R^2	0.705	0.926	0.986
Intra-particle diffusion	K_{id1} (mg/g.min$^{1/2}$)	0.880	1.052	1.028
	C_1 (mg/g)	1.498	2.785	7.594
	R_1^2	0.979	0.943	0.974
	K_{id2} (mg/g.min$^{1/2}$)	0.016	0.122	0.316
	C_2 (mg/g)	5.856	9.666	16.294
	R_2^2	0.584	0.891	0.953

Where C_e is the equilibrium concentration (mg/L), q_m is the monolayer adsorption capacity (mg/g) and K_L is the constant related to the free adsorption energy (Langmuir constant, L/mg).

q_m and K_L are determined from the slope and the intercept of the plot of C_e/q_e versus C_e. Equilibrium parameter for Langmuir isotherm called separation factor (R_L) was expressed as Eq. 10. The values of this parameter indicate the shape of the isotherm which: $R_L > 1$ is unfavorable, $R_L = 1$ is linear, $R_L = 0$ is irreversible, and finally $0 < R_L < 1$ is favorable.

$$R_L = \frac{1}{1 + K_L C_0} \qquad (10)$$

- *Freundlich isotherm*

For Freundlich isotherm model, the linear form is presented by Eq. 11.

$$\ln q_e = n \ln C_e + \ln K_F \qquad (11)$$

Where K_F is the constant indicative of the adsorption capacity of the adsorbent ($(mg/g)/(mg/L)^n$) and n constant shows adsorption intensity of dye onto the adsorbent. For a suitable adsorption system, n value varies between 0 and 1. K_F and n are determined by the intercept and the slope is obtained from the slope of the linear plot of $\ln q_e$ against $\ln C_e$.

- *Temkin Isotherm*

Eq. 12 presents linear form for Temkin isotherm model.

$$q_e = B_T \ln C_e + B_T \ln A_T \qquad (12)$$

Where B_T is the constant related to the heat of adsorption (mg/g), A_T is Temkin isotherm constant (L/min). The two constants (B_T, A_T) are calculated by the plot of q_e against $\ln C_e$.

Because of the inherent bias resulting from linearization of isotherm models, the non-linear regression Root Mean Square Error (RMSE) (Eq. 13) and Chi-Squares (χ^2) (Eq. 14) test are used as criteria for the fitting quality. The smaller RMSE, χ^2 values indicates the better curve fitting [45].

$$RMSE = \sqrt{\frac{1}{N-2} \cdot \Sigma_1^N (q_{e,exp} - q_{e,cal})^2} \qquad (13)$$

$$\chi^2 = \sum_1^N \frac{(q_{e,exp} - q_{e,cal})^2}{q_{e,cal}} \qquad (14)$$

Where $q_{e,exp}$ (mg/g) is the uptake experimental, $q_{e,cal}$ (mg/g) the calculated value of uptake using a model and N the number of observations in the experiment (the number of data points).

The calculated parameters characteristics of each isotherm model are given in **Table 2**. It can be seen from the results illustrated in **Table 2**, that Langmuir isotherm fits better than Freundlich and Temkin isotherms with higher determination coefficients ($R^2 \sim 0.99$) and the smaller RMSE, χ^2 values indicates the better curve fitting. For all studied temperatures, R_L values vary between 0.03 and 0.4, and are belonging in the range of 0-1 indicating that MB adsorption onto RSF is a favorable process.

Table 2 . Isotherm parameters obtained for adsorption of MB onto RSF (constants and error analysis).

Isotherms	Parameters	Temperature (K)		
		295	**303**	**313**
Langmuir	R^2	**0.999**	**0.999**	**0.998**
	K_L(L/mg)	0.269	0.254	0.275
	q_m(mg/g)	20.462	25.265	27.670
	RMSE	0.426	0.356	0.755
	χ^2	0.072	0.031	0.125
Freundlich	R^2	0.874	0.900	0.895
	K_F((mg/g)/(mg/L)^n)	5.600	6.243	6.650
	n	0.348	0.388	0.414
	RMSE	2.786	3.561	4.556
	χ^2	2.108	2.610	3.484
Temkin	R^2	0.968	0.963	0.972
	B_T(mg/g)	3.701	4.921	5.422
	A_T(L/min)	4.048	3.401	3.269
	RMSE	1.123	1.264	1.635
	χ^2	0.472	0.350	0.508

III.9. Thermodynamic study

The various thermodynamic parameters, standard free energy ($\Delta G°$), standard enthalpy ($\Delta H°$) and standard entropy ($\Delta S°$) were determined using Eq. 15 and Eq. 16 [46]. The $\Delta H°$ and $\Delta S°$ values are obtained from the slope and intercept of Van't Hoff plots of ln K_d versus 1/T, respectively.

$$\Delta G° = -R\,T\,\ln K_d \qquad (15)$$

$$\ln K_d = \frac{\Delta S°}{R} - \frac{\Delta H°}{RT} \qquad (16)$$

Where R is the universal gas constant (8.314 J/mol.K), T the absolute temperature in Kelvin and K_d is the distribution coefficients. K_d values are obtained from plotting ln (q_e/C_e) versus C_e and extrapolating to zero [44].

A calculation of fundamental thermodynamic parameters ($\Delta G°$, $\Delta H°$ and $\Delta S°$) is represented in **Table 3**. We notice that, the negative values of $\Delta G°$ for all temperatures indicate spontaneous nature of adsorption. $\Delta G°$ values were between -20 and 0 kJ/mol which indicate a physical adsorption process [34] The positive values of $\Delta H°$ and $\Delta S°$ indicate the endothermic nature of adsorption interaction and an increase in randolness at

RSF/MB solution interface, respectively [47].

III.10. Performances of the prepared RSF

It is instructive for a comparative purpose to report the values of the adsorption capacity of some adsorbents available in the literature. In **Table 4**, it's given the different values of the Langmuir maximum adsorption capacity (q_m) of different low-cost adsorbents cited in previous works. We can see that the MB adsorption observed in this work is well positioned with respect to other research. For our study, the maximum adsorption capacity of MB at 313 K onto RSF (27.67 mg/g) is relatively interesting compared to other adsorbents.

IV. Conclusion

This study has focused on the application of low-cost and easily available adsorbent in wastewater treatment. A natural waste of sorghum was used in adsorption without any activation to retain methylene blue MB dye from aqueous solutions. The adsorption process was studied as a function of selected parameters. It has been noticed that, the MB removal increases with increasing pH solution, initial MB concentration and decreasing adsorbent dose and salt concentration. The results of the kinetic study show that, the adsorption process

Table 3. Adsorption thermodynamic parameters for adsorption of MB onto RSF.

Temperature (K)	ln K$_d$	$\Delta G°$ (kJ/mole)	Van't Hoff equation	$\Delta H°$ (kJ/mole)	$\Delta S°$ (J/mole.K)
295	1.0465	-2.566			
303	1.3149	-3.312	y = -2068,7x + 8,0883 R^2 = 0,9489	17.199	67.246
313	1.4542	-3.784			

A LJEST

Table 4. Comparison of Langmuir maximum equilibrium capacity for MB ontoother low-cost adsorbent

Adsorbent	Maximum adsorption capacity q_m(mg/g)	References
Spend coffee grounds	18.7	**[3]**
Sawdust from saw mills	76.92	**[31]**
Palm tree	29.5	**[32]**
Sugarcane bagasse	30.7	**[47]**
Walnut sawdust	58.17	**[48]**
Cheery tree sawdust	39.84	
Oak tree sawdust	29.94	
Pitch-pine sawdust	27.78	
Modified wheat bran	25.18	**[49]**
Wheat shells	21.5	**[50]**
Banana peels	20.8	**[51]**
Orange peels	18.6	
Modified rice husk	29.15	**[52]**
Aleppo pine cones	93.57	**[53]**
Raw Sorghum fibers RSF	**27.67**	**This study**

obeyed to the pseudo-second order model. The adsorption isotherm study shows that the adsorption isotherm of MB onto RSFfollows the Langmuirmodel and the maximum adsorption capacity corresponding was 27.78 mg/g at 313 K. The process was endothermic with positive values of enthalpy. Randomness increased at the interface and the process was found to be spontaneous. The results of the present investigation showed that RSF is a potentially useful adsorbent for the adsorption of dyes, an issue of environmental concern. The comparison of the adsorption capacity of the prepared adsorbent with other adsorbents shows its attractive properties from industrial and economic interests.

V. References

1. Namasivayam,C.;Kavitha, D. Removal of Congo red from water by adsorption onto activated carbon prepared from coir pith, an agricultural solid waste. *Dye Pigment*. 54 (2002) 47-58.
2. Katheresan, V.; Kansedo, J.; Lau, S.Y. Efficiency of various recent waste water dye removal methods. A review.*Journal of Environmental Chemical Engineering*. 6 (2018), 4676-4697.
3. Franca, A.S.; Oliveira, L.S.; Ferreira, M.E. Kinetics and equilibrium studies of methylene blue adsorption by spent coffee grounds. *Desalination*. 249 (2009) 267-272.
4. Daoud, M.; Benturki O.; Girods, P.; et al. Adsorption ability of activated carbons from Phoenix dactylifera rachis and Ziziphus jujube stones for the removal of commercial dye and the treatment dye stuff wastewater. *Microchemical journal*. doi.org/10.1016/j.micro.2019.05.022.

5. Weng, C.H.; Pan, Y.F. Adsorption of a cationic dye (methylene blue) onto spent activated clay. *Journal of Hazardous Materials*. 144 (2007) 355-362.
6. Papic, S.; Koprivanac, N.; Bozic, A.L.; Meters, A. Removal of some Reactive Dyes from Synthetic Waste water by Combined Al(III) Coagulation/Carbon Adsorption Process. *Dyes Pigment*. 62 (2004) 291-298.
7. Kobya, M.; Can, O.T.; Bayramoglu, M. Treatment of textile wastewaters by electrocoagulation using iron and aluminum electrodes. *Journal of Hazardous Materials*. 100 (2003) 163-178.
8. Zereshki, S.; Daraei, P.; Shokri, A. Application of edible paraffin oil for cationic dye removal from water using emulsion liquid membrane. *Journal of Hazardous Materials*. 356 (2018) 1-8.
9. Meric, S.; Selcuk, H.; Belgiorno, V. Acute toxicity removal in textile finishing wastewater by Fenton's oxidation, ozone and coagulation-flocculation processes. *Water Research*. 39 (2005) 1147-1153.
10. Saeed, A.; Sharif, M.; Iqbal, M. Application potential of grapefruit peel as dye sorbent: kinetics, equilibrium and mechanism of crystal violet adsorption. *Journal of Hazardous Materials*. 179 (2010) 564-72.
11. Mohan, S.V.; Ramanaiah, S.V.; Sarma, P.N. Biosorption of direct azo dye from aqueous phase onto Spirogyra sp. I02: Evaluation of kinetics and mechanistic aspects. *Biochemical Engineering Journal*. 38 (2008) 61-69.
12. Chatterjee, S.; Chatterjee, B.P.; Guha, A.K. Adsorptive removal of Congo red, a carcinogenic textile dye by chitosan hydrobeads: Binding mechanism, equilibrium and kinetics. *Colloids and Surfaces A: Physicochemical and Engineering Aspects*. A 299 (2007) 146-152.
13. Saleh, T.A.; Gupta, V.K. Photo-catalyzed degradation of hazardous dye methyl orange by use of a composite catalyst consisting of multi-walled carbon nanotubes and titanium dioxide. *Journal of Colloid and Interface Science*. 371 (2012) 101-106.

14. Komaros, M.; Lyberatos, G. Biological treatment of wastewater from a dye manufacturing company using à trickling filter. *Journal of Hazardous Materials.* 136 (2006) 95-102.

15. Adegoke, K.A.; Bello, O.S. Dye sequestration using agricultural wastes as adsorbents. *Water Research and Industry.* 12 (2015) 8-24.

16. Ansari, R.; Seyghali, B. Application of wood sawdust modified with cationic surfactants for efficient removal of acidic dyes from aqueous solutions: kinetic and thermodynamic studies. *European Chemical Bulletin.* 2(7) (2013) 499-506.

17. Deng, S.; Bai, R.; Chen, J.P. Behaviors and mechanisms of copper adsorption on hydrolyzed polyacrylonitrile fibers. *Journal of Colloid and Interface Science.* 260 (2003) 265-272.

18. Shubha, K.P.; Raji, C.; Anirudhan, T.S. Immobilization of heavy metals from aqueous solutions using polyacrylamide grafted hydrous tin (IV) oxide gel having carboxylate functional groups. *Water Research.* 35 (2001) 300-310.

19. Nekouei, F.; Nekouei, S.; Tyagi, I.; Gupta, V.K. Kinetic, thermodynamic and isotherm studies for acid blue 129 removal from liquids using copper oxide nanoparticle-modified activated carbon as a novel adsorbent. *Journal of Molecular Liquids.* 201 (2015) 124-133.

20. Dehghani, M.H.; Taher, M.M.; Bajpai, A.K.; Heibati, B.; Tyagi, I.; Asif, M.; Agarwal, S.; Gupta, V.K. Removal of noxious Cr(VI) ions using single-walled carbon nanotubes and multi-walled carbon nanotubes. *Chemical Engineering Journal.* 279 (2015), 344-352.

21. Gupta, V.K.; Suhas.; Nayak, A.; Agarwal, S.; Chaudhary, M.; Tyagi, I. Removal of Ni (II) ions from water using scrap tire. *Journal of Molecular Liquids.* 190 (2014) 215-222.

22. Robati, D.; Mirza, B.; Rajabi, M.; Moradi, O.; Tyagi, I.; Agarwal, S.; Gupta, V.K. Removal of hazardous Dyes-BR 12 and methyl orange using graphene oxide as an adsorbent from aqueous phase. *Chemical Engineering Journal.* 268 (2015) 28-37.

23. Sahmoune, M.N.; Louhab, K.; Boukhiar, A. Biosorption of Cr(III) from aqueous solutions using bacterium biomass Streptomyces Rimosus. *International Journal of Environmental Research,.* 3(2) (2009) 229-238.

24. Kadirvelu, K.; Kavipriya, M.; Karthika, C.; Radhika, M.; Vennilamani, N.; Pattabhi, S. Utilization of various agricultural wastes for activated carbon preparation and application for the removal of dyes and metal ions from aqueous solutions. *Bioresource Technology.* 87 (2003) 129-132.

25. Largitte L.; Brudey T.; Tant, T.; Couespe, lP.; Dumesnil, Lodewyckx, P. Comparison of the adsorption of lead by activated carbons from three lignocellulosic precursors: Review. *Microporous Mesoporous Materials.* 219 (2016) 265-275.

26. Gherbia, A.; Hurel, C.; Chergui, A.; Yeddou, A. R.; Selatnia, A.; Nadjemi, B. Adsorptive removal of methylene blue by low cost agricultural waste: *Deglabeida*Dates Stones in a Fixed-bed dynamic column. *Research Journal of Chemistry and Environment.* 23 (2019) 74-80.

27. Hokkanen, S.; Bhatnagar, A.; Sillanpää, M. A review on modification methods to cellulose-based adsorbents to improve adsorption capacity: Review. *Water Research.* 91 (2016) 156-173.

28. Sahmoune, M.N.; Yeddou, A.R. Potential of sawdust materials for the removal of dyes and heavy metals: examination of isotherms and kinetics. *Desalination Water Treatment.* 57 (2016) 24019-24034.

29. Rafatullaha, M.; Sulaimana, O.; Hashima, R.; Ahmad, A. Adsorption of methylene blue on low-cost adsorbents: A review. *Journal of Hazardous Materials.* 177 (2010) 70-80.

30. Salleh, M.A.M.; Mahmoud Khalid, D.; Abdul Karim, W.A.W., Idris, A. Cationic and anionic dye adsorption by agricultural solid wastes: A comprehensive review. *Desalination* 28 (2011) 1-13.

31. Markandeya Singh, A.; Shukla, S.P.; Mohan, D.; Singh, N.B.; Bhargava, D.S.; Shukla, R.; Pandey, G.; Yadav, V.P.; Kisku, G.C. Adsorptive capacity of sawdust for the adsorption of MB dye and designing of two-stage batch adsorber. *Cogent Environmental Science.* 1(2015) 1-16.

32. Belala, Z.; Jeguirim, M.; Belhachemi, M.; Addoun, F.; Trouvé, G. Biosorption of basic dye from aqueous solutions by Date Stones and Palm-Trees Waste: Kinetic, equilibrium and thermodynamic studies. *Desalination.* 271 (2011) 80-87.

33. Han, R.; Zou, W.; Yu, W.; Cheng, S.; Wang, Y.; Shi, J. Biosorption of methylene blue from aqueous solution by fallen phoenix tree's leaves. *Journal of Hazardous Materials.* 141 (2007) 156-162.

34. Moussavi, G.; Khosravi, R. The removal of cationic dyes from aqueous solutions by adsorption onto pistachio hull waste. *Chemical Engineering Research and Design.* 89 (2011) 2182-2189.

35. Boudries, N.; Belhaneche, N.; Nadjemi, B.; Deroanne, C.; Mathlouthi, M.; Roger, B.; Sindic, M. Physicochemical and functional properties of starches from sorghum cultivated in the Sahara of Algeria. *Carbohydrate Polymers.* 78 (2009) 475-480.

36. Abbas, M.; Kaddour, S.; Trari, M. Kinetic and equilibrium studies of cobalt adsorption on apricot stone activated carbon. *Journal of Industrial and Engineering Chemistry.* V20 (2014) 745-751.

37. Oladoja, N.A.; Aboluwoye, C.O.; Oladimeji, Y.B.; Ashogbon, A.O.; Otemuyiwa, I.O. Studies on castor seed shell as a sorbent in basic dye contaminated wastewater remediation. *Desalination.* 227 (2008) 190-203.

38. Suteu, D.; Biliuta, G.; RusuL.; Coseri, S.; Nacu, G. Cellulose cellets as new type of adsorbent for the removal of dyes from aqueous media. *Environmental engineering and management journal.* 14 (3) (2015) 525-532.

39. Chen, H.; Zhao, J.; Dai, G. Silkworm exuviae-A new non-conventional and low-cost adsorbent for removal of methylene blue from aqueous solutions. *Journal of Hazardous Materials.* 186 (2011) 1320-1327.

40. Han, X.; Wang, W.; Ma, X. Adsorption characteristics of methylene blue onto low cost biomass material lotus leaf. *Chemical Engineering Journal.* 171 (2011) 1-8.

41. Yeddou-Mezenner, N. Kinetics and mechanism of dye biosorption onto an untreated antibiotic waste. *Desalination.* 262 (2010) 251-259.

42. Özacar, M.; Şengil, İ.A. Adsorption of metal complex dyes from aqueous solutions by pine sawdust. *Bioresource Technolgy.* 96 (2005) 791-795.

43. Lagergren, S. About the theory of so-called adsorption of soluble substance. *Kungliga Svenska Vetenskapsakademiens Handlingar.* 24 (1898) 1-39.

44. Tran, H.N.; YouS-J.; Hosseini-Bandegharaei, A.; Chao, H-P. Mistakes and inconsistencies regarding adsorption of contaminants from aqueous solutions: A critical review. *Water Research.* 120 (2017) 88-116.

45. Abbas, M.; TrariM. Kinetic, Equilibrium and Thermodynamic Study on the Removal of Congo Red from Aqueous Solutions by Adsorption onto Apricot Stone. *Process Safety Environmental.* 98 (2015) 424-436.

46. Akar, S.T.; Özcan, A.S.; Akar, T.; Özcan, A.; Kaynak, Z. Biosorption of a reactive textile dye from aqueous solutions utilizing an agro-waste. *Desalination.* 249 (2009) 757-761.

47. Zhang, Z.; O'HaraI, .M.; Kent, G.A.; Doherty, W.O.S. Comparative study on adsorption of two

cationic dyes by milled sugarcane bagasse. *Industrial Crops and Products.* 42 (2013) 41-49.

48. Ferrero, F. Dye removal by low cost adsorbents: Hazelnut shells in comparison with wood sawdust. *Journal Hazardous Materials.* 142 (2007)144-152.

49. Yao, S.; Lai, H.; Shi, Z. Biosorption of methyl blue onto tartaric acid modified wheat bran from aqueous solution. *Iran Journal Environmental Health Science Engineering.* 9 (2012) 1-6.

50. Bulut, Y.; Aydın, H. A kinetics and thermodynamics study of methylene blue adsorption on wheat shells. *Desalination.* 194 (2006) 259-267.

51. Annadurai, G.; Juang, R-S. ; Lee, D-J. Use of cellulose-based wastes for adsorption of dyes from aqueous solutions. *Journal Hazardous Materials.* B92 (2002) 263-274.

52. Lee, S-M.; Ong, S-T. Oxalic Acid Modified Rice Hull as a Sorbent for Methylene Blue Removal. *APCBEE Procedia.* 9 (2014) 165-169.

53. Elmoubarki, R.; Moufti, A.; Tounsadi, H.; Mahjoubi, F.Z.; Farnane, M.; Machrouhi, A.; Elhalil, A.; Abdennouri, M.; Zouhri, A.; Barka, N. Kinetics and thermodynamics study of methylene blue adsorption onto Aleppo pine cones. *Journal of Materials and Environmental Science.* 7 (8) (2016) 2869-2879.

Please cite this Article as:
Sifoun N., Yeddou A-R., Nouri L-H., Chergui A., Nadjemi B., Kinetic and thermodynamic studies of methylene blue adsorption on sorghum stems, ***Algerian J. Env. Sc. Technology****, 6***:3(2020) 1526-1536**